

# PHY 982 Homework 3

John Ash, Mengzhi Chen, Tong Li, Jason Surbrook

March 22, 2018

## 1 Choice of beam energies and potentials

The  $^{12}\text{C}(\text{d}, \text{p})^{13}\text{C}$  reaction is discussed in this work. The Coulomb barrier between  $^{12}\text{C}$  and deuteron is about 2.03 MeV. Two deuteron beam energies are studied, one is 2.84 MeV near the Coulomb barrier; another one is 4.51 MeV which is about 2 times the barrier. Ref. [1] shows that, in the energy range from 1.8 to 6.1 MeV, there is a considerable contribution from compound nucleus formation. Therefore, our calculations using FRESKO are expected to yield less satisfying agreement with experiment for the lower beam energy and for large angles.

Optical potentials are needed that described the incoming and outgoing distorted waves. These are interactions between the following pairs: ( $^{12}\text{C}$ , d) [2], ( $^{12}\text{C}$ , p) [3] and ( $^{13}\text{C}$ , p). For the potential of ( $^{13}\text{C}$ , p), we cannot find an appropriate one in the energy range we study, so we use the potential of ( $^{12}\text{C}$ , p) at the relevant energies instead. For the deuteron wavefunction, the binding for the proton and neutron is described by a simple Gaussian potential

$$V_{np}(r) = -72.15e^{-(r/1.484)^2}. \quad (1)$$

which reproduces a bound s-state at 2.2 MeV.

The neutron that is transferred in the reaction is expected to occupy a  $1p_{1/2}$  orbit with an experimental single-particle binding energy of 4.946 MeV. The FRESKO is set to dynamically adjust the Woods-Saxon depth for  $^{13}\text{C}$  to reproduce this energy.

## 2 Results of DWBA post-form calculations

In a transfer reaction  $A(\text{d}, \text{p})B$  showed in Fig. 1, by introduction the auxiliary potential  $U_f(R_2)$ , the transfer T-matrix has a formula [4]

$$T_{\text{post}} = \langle \phi_{nA} \chi_{pB}^{(-)} | V_{np}(r_1) + U_{pA}(r_p) - U_f(R_2) | \Psi_1^{(+)}(\vec{r}_1, \vec{R}_1) \rangle, \quad (2)$$

where  $\phi_{nA}$  and  $\chi_{pB}$  are bound states wave-functions. Under first-order DWBA, it becomes

$$T_{\text{post}}^{\text{DWBA}} = \langle \phi_{nA} \chi_{pB}^{(-)} | V_{np}(r_1) + U_{pA}(r_p) - U_f(R_2) | \phi_{np} \chi_{dA} \rangle. \quad (3)$$

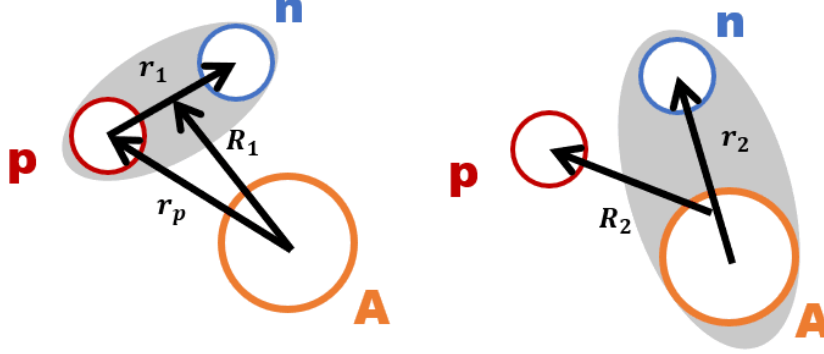


Figure 1: Coordinates used in one neutron transfer reaction.

Besides that, we still need information for the auxiliary potential  $U_f(R_2)$ . It's usually chosen as  $U_{pB}(R_2)$  fitted from elastic scattering. We name  $V_{np}(r_1)$  as binding potential and the rest two remnants.

Here are three different handling methods we used in our calculations.

1. Zero range (ZR) approximation: Remnants are neglected;  $V_{np}(r_1)$  is considered as a local interaction with strength  $D_0$ . Correspondingly, the T-matrix becomes

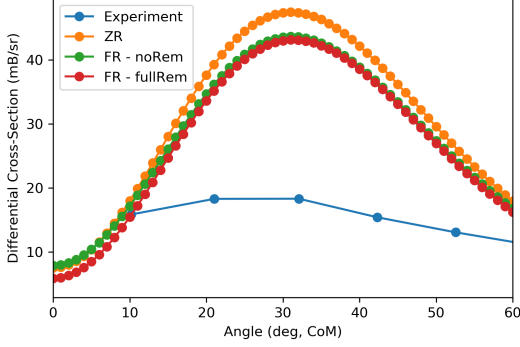
$$T_{\text{post}}^{\text{ZR-DWBA}} = D_0 \langle \phi_{nA}(R_1) \chi_{pB}^{(-)} | \chi_{dA}(R_1) \rangle. \quad (4)$$

It now relies on  $R_1$  only, which simplifies calculation.

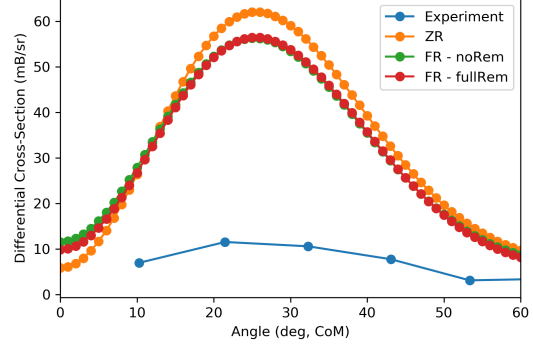
2. First-order DWBA: finite-range interactions, without and with full complex remnant. The former abandons the remnants but the latter keeps them. The nonlocality of  $V_{np}(r_1)$  is preserved in both.

Our results are generated with radius  $r_{\text{match}} = 60$  fm, partial waves up to  $j_{\text{max}} = 55$  (in units of  $\hbar$ ) and step size  $\text{rintp} = 0.2$  fm. Under zero-range approximation, coefficient  $D_0$  is chosen to be 125.35 MeV, the same as FRESKO's recommendation. To test the convergence, these values are modified up to  $r_{\text{match}} = 80$  and  $j_{\text{max}} = 70$  and down to  $\text{rintp} = 0.01$  for the full complex remnant case. The differential cross sections deviate  $< 2\%$  between calculation initializations. Furthermore, as long as  $\text{rintp} > 0.05$ , the deviation from primary initializations is  $< 0.5\%$ , so  $< 2\%$  is a conservative limit to stability. Other grid and strength parameters like non-local range  $\text{rnl}$  and  $\text{centre}$  are adapted from FRESKO's suggestions, while  $\text{rnl}$  is set to 0.5 fm larger than the largest  $\text{rnl}$  suggestion.

The post-form results together with experimental data [1] are presented in Fig. 2. In both energy scales, all three differential cross sections fit well with experiment in



(a) Beam energy is 2.84 MeV.



(b) Beam energy is 4.51 MeV.

Figure 2: Forward-angled differential cross sections calculated under: 1) zero-range approximation (ZR); 2) first-order DWBA in post form, finite range, without remnant (FR - noRem); 3) first-order DWBA in post form, finite range, with full complex remnant (FR - fullRem), as well as experimental data.

shape. Also, the agreement is better for 4.51 MeV case, as it gives more direct reactions than the 2.84 MeV case. We can see that ZR approximation gives result deviates most from experiment because it applies the roughest approximation. It looks DWBA with or without remnants yield very similar results. This may be anticipated because of the similarity in  $U_{pA}$  and  $U_{pB}$  that they almost cancel each other in Eq. 3. However, DWBA with remnants is closer to experiment, which is not surprising.

### 3 Results of prior-form DWBA calculations

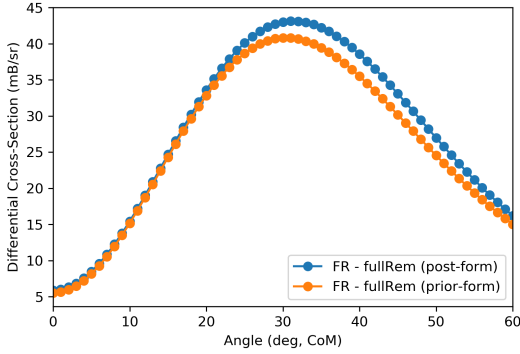
In a transfer reaction  $A(d,p)B$ , the transfer T-matrix has a prior-form formula [4]

$$T_{\text{prior}} = \langle \Psi_2^{(-)}(\vec{r}_2, \vec{R}_2) | V_{nA}(r_n) + U_{pA}(r_p) - U_{dA}(R_1) | \phi_{np} \chi_{dA} \rangle, \quad (5)$$

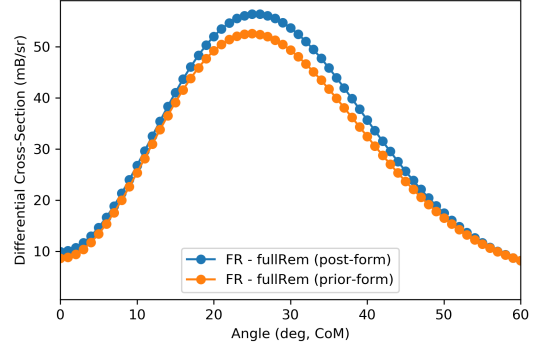
where  $\phi_{np}$  and  $\chi_{dA}$  are bound states wave-functions,  $\vec{r}_n = \vec{r}_p + \vec{r}_1$ , and  $U_{dA}(R_1)$  is the auxiliary potential we choose. Under first-order DWBA, it becomes

$$T_{\text{prior}}^{\text{DWBA}} = \langle \phi_{nA} \chi_{pB}^{(-)} | V_{nA}(r_n) + U_{pA}(r_p) - U_{dA}(R_1) | \phi_{np} \chi_{dA} \rangle, \quad (6)$$

The differential cross sections of  $^{12}\text{C}(d, p)^{13}\text{C}$  calculated in both post and prior forms are given in Fig. 3. First-order DWBA with finite-range interactions and full complex remnant is used in both calculations. The convergence of calculations in prior form is checked in the same way as we discussed in Sec. 2. Variables *rnl* and *centre* are chosen based on FRESCO's recommendations. As shown in Fig. 3, the results from post- and



(a) Beam energy is 2.84 MeV.



(b) Beam energy is 4.51 MeV.

Figure 3: Forward-angled differential cross sections calculated under: 1) first-order DWBA in post form, finite range, with full complex remnant [FR - fullRem (post-form)]; 2) first-order DWBA in prior form, finite range, with full complex remnant [FR - fullRem (prior-form)].

prior-form calculations are close to each other, which agrees with the fact that post and prior forms theoretically give the same results in the first-order DWBA.

It is worth mentioning that the recommended  $rnl$ , which represents the non-local range, is larger in prior form (12.50 fm) than that in post form (5.6 fm). In post form (Eq. 3)  $U_{pA}(r_p)$  and  $U_{pB}(R_2)$  are close to each other as nuclei A and B are very similar. Thus, the operator in Eq. 3 is approximately  $V_{np}(r_1)$ , which has a very short range. However, in prior form (Eq. 6)  $U_{pA}(r_p)$  and  $U_{dA}(R_1)$  cannot cancel each other as the elastic scatterings of deuteron on A and proton on A are very different. Thus, the operator in Eq. 6 has a longer range which comes from optical potentials  $U_{pA}(r_p)$  and  $U_{dA}(R_1)$ . A larger  $rnl$  in prior-form calculation also leads to a longer runtime.

## 4 Extraction of spectroscopic factor

As is normal, the spectroscopic factor is extracted by comparing the theory to the data at the first peak in the angular distribution [5], as we expect that the reaction is mostly direct at the forward angle. The spectroscopic factors at beam energies 2.84 MeV and 4.51 MeV are given in Table 1. The angle of first peak  $\theta_p$  and corresponding differential cross section  $\sigma^{\text{DWBA}}$  is given by the first-order DWBA calculations in post form with finite-range interactions and full complex remnant (see Sec. 2).  $\sigma^{\text{exp}}$  is obtained by spline interpolation of experimental data. The spectroscopic factors we extract are energy-dependent, which is expected because Ref. [1] shows that compound nucleus formation has a considerable contribution in the reaction mechanism.

Table 1: Spectroscopic factors  $S$  extracted from  $^{12}\text{C}(d, p)^{13}\text{C}$ .  $\theta_p$  is the angle of the first peak, and  $\sigma^{\text{exp}}$  and  $\sigma^{\text{DWBA}}$  are corresponding differential cross sections obtained from experimental data and post-form DWBA calculation, respectively.

Beam energy (MeV)	2.84	4.51
$\theta_p$ (degree)	31	25
$\sigma^{\text{exp}}$ (mb/sr)	18.49	11.57
$\sigma^{\text{DWBA}}$ (mb/sr)	43.14	56.40
$S = \sigma^{\text{exp}}/\sigma^{\text{DWBA}}$	0.4286	0.2051

## References

- [1] T. W. Bonner, J. T. Eisinger, Alfred A. Kraus, and J. B. Marion. Cross section and angular distributions of the  $(d, p)$  and  $(d, n)$  reactions in  $^{12}\text{C}$  from 1.8 to 6.1 MeV. *Phys. Rev.*, 101:209–213, Jan 1956.
- [2] Haixia An and Chonghai Cai. Global deuteron optical model potential for the energy range up to 183 MeV. *Phys. Rev. C*, 73:054605, May 2006.
- [3] M.B.Chadwick and P.G.Young. Proton nuclear interactions up to 250 MeV for radiation transport simulations of particle therapy. *Proc.Int. Particle Therapy Mtg. and PTCOG XXIV*, Apr 1996.
- [4] Ian J Thompson and Filomena M Nunes. Nuclear reactions for astrophysics: principles, calculation and applications of low-energy reactions. pages 150–157, 2009.
- [5] X. D. Liu, M. A. Famiano, W. G. Lynch, M. B. Tsang, and J. A. Tostevin. Systematic extraction of spectroscopic factors from  $^{12}\text{C}(d, p)^{13}\text{C}$  and  $^{13}\text{C}(p, d)^{12}\text{C}$  reactions. *Phys. Rev. C*, 69:064313, Jun 2004.